Do the One-Electron Oxidized Derivatives of Some Six-Coordinate Low-Spin Iron(III) Porphyrins Feature Strong Metal−Ligand Ferromagnetic Coupling?

Jeanet Conradie[†,‡] and Abhik Ghosh*[,†]

Department of Chemistry, Faculty of Science, University of Tromsø, N-9037 Tromsø, Norway, and Department of Chemistry, University of the Free State, 9300 Bloemfontein, Republic of South Africa

Received: March 20, 2003

It has been recognized for some time that the high-valent complex $[Fe(TPP)(1\text{-}MeIm)_2]^{2+}$ (TPP = *meso*-tetraphenylporphyrin, 1-MeIm = 1-methylimidazole) exhibits an S = 1 ground state and has been described as a low-spin Fe(III) porphyrin π-cation radical with strong metal−porphyrin ferromagnetic coupling. Because strong metal−ligand ferromagnetic coupling is quite unusual, a DFT investigation of two truncated and symmetrized models of this complex, namely, $[Fe(P)(Py)_2]^{2+}$ and $[Fe(P)(ImH)_2]^{2+}$, was carried out. The results indicate that the ground-state electronic configurations may be described as low-spin Fe(IV)-like, with varying degrees of metal-to-porphyrin spin delocalization, which provides a natural explanation for the experimentalists' somewhat unusual description of the electronic structure of $[Fe(TPP)(1\text{-}MeIm)_2]^{2+}$.

Introduction

High-valent transition metal intermediates are involved in a variety of oxidative processes of biological and industrial importance.[1,2] Accordingly, much effort has gone into characterizing the geometric and electronic structures as well as the chemical reactivity of such species, of which high-valent iron porphyrins have been particularly intensively studied. Density functional theory (DFT)[3−5] calculations have played a major role in this area and have been applied to many metalloporphyrin π-cation radicals,[6] peroxidase compound I and compound II intermediates,[7−15] high-spin iron(III) porphyrin π-cation radicals,[16] iron(V)-nitrido porphyrins,[17] manganese(IV) and manganese(V) porphyrin intermediates,[16,18] high-valent iron and manganese corroles,[15,19,20,21] Ni(III) porphyrins,[22,23] and Cu(III) corroles.[24] However, one class of high-valent metalloporphyrins for which electronic structures and unique magnetic properties remain to be adequately elucidated comprises the one-electron oxidized derivatives of six-coordinate low-spin iron(III) porphyrins.[25]

Six-coordinate iron porphyrinoids occur at the active sites of a variety of biomolecules such as cytochromes *b* and the enzymes containing the so-called green hemes.[26−33] Depending on the nature of the axial ligands and of the porphyrinoid, the electronic configuration for the iron(III) oxidation state varies from $(d_{xz},d_{yz})^3(d_{xy})^2$ to $(d_{xz},d_{yz})^4(d_{xy})^1$, leading to wide variations in the structural (conformational) and electronic (spectroscopic) properties of these molecules.[34−37] DFT calculations on six-coordinate low-spin ferrihemes [i.e., iron(III) porphyrins] with N-heteroaromatic axial ligands have provided a reasonably satisfactory theoretical characterization of these two different spin states.[38,39] In contrast, as indicated above, the electronic structures of the one-electron oxidized derivatives of such ferrihemes have remained something of a mystery for the past 20 years.

The electronic structure of $[Fe(TPP)(1\text{-}MeIm)_2]^{2+}$ (TPP = *meso*-tetraphenylporphyrin, 1-MeIm = 1-methylimidazole) was thought of as involving a pair of noninteracting $S = {}^1/_2$ centers, namely, the low-spin Fe(III) center and a porphyrin radical.[25] Subsequently, arguments based on the NMR chemical shifts of the phenyl protons led to an electronic structural description involving an S = 1 ground state resulting from strong *ferromagnetic* coupling of the low-spin Fe(III) center and a porphyrin radical.[40] To put this result in perspective, we note that metal−ligand ferromagnetic coupling results from orthogonal metal- and ligand-based magnetic orbitals and is rarely strong. Perhaps the best-known bioinorganic example of such spin coupling is horseradish peroxidase compound I, which is an $S = {}^3/_2$ species with a ferromagnetically coupled Fe(IV)−oxo center and a porphyrin radical.[1]

Interestingly, the nature of metal−ligand spin coupling in $[Fe(TPP)(1\text{-}MeIm)_2]^{2+}$ appears to be quite different from that in $[Fe(porphyrinato)(2\text{-}MeIm)_2]^{2+}$ derivatives, which have been studied recently by Nakamura and co-workers.[41,42] The latter derivatives, which are expected to have strongly ruffled porphyrin ligands, were found to exhibit S = 0 ground states, which was reasonably attributed to metal−porphyrin antiferromagnetic coupling mediated by an $Fe(d_{xy})$−porphyrin(a_{2u}) orbital overlap that is specifically symmetry-allowed in a ruffled porphyrin.[34−38]

What accounts for the strong ferromagnetic coupling for $[Fe(TPP)(1\text{-}MeIm)_2]^{2+}$? To find out, we have carried out DFT calculations on different spin states of two truncated and symmetrized models of $[Fe(TPP)(1\text{-}MeIm)_2]^{2+}$, namely, $[Fe(P)(Py)_2]^{2+}$ (D_{2d}, S = 1, Py = pyridine), and on two conformations of $[Fe(P)(ImH)_2]^{2+}$ (C_2, S = 1, ImH = imidazole) (Figure 1). We believe that the results provide some insights into this question.

Methods

All calculations have been carried out with DFT as implemented in the ADF2000 program system,[43] the gradient-corrected PW91 exchange-correlation functional, Slater-type triple-ζ plus polarization basis sets, full geometry optimizations with appropriate symmetry constraints, and tight SCF and geometry optimization convergence criteria and fine integration

* Corresponding author. E-mail: abhik@chem.uit.no.
† University of Tromsø.
‡ University of the Free State.

10.1021/jp030354n CCC: $25.00
Published on Web 06/11/2003

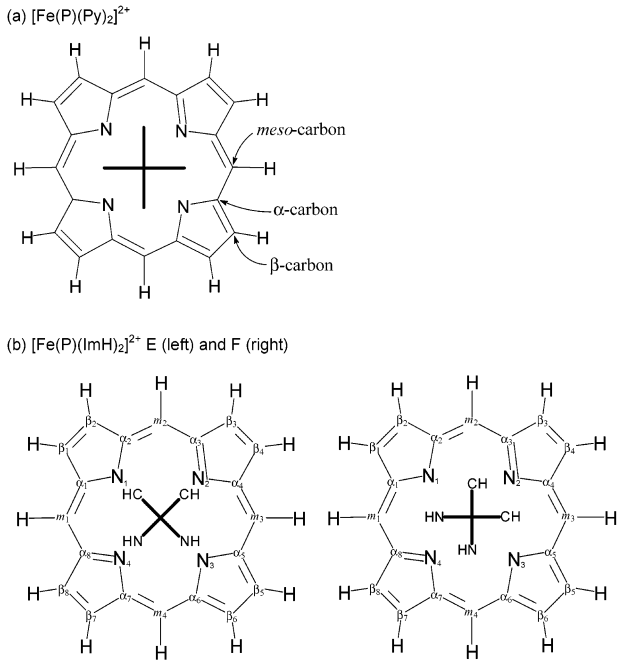

Figure 1. Top views of the molecular structures of (a) $[Fe(P)(Py)_2]^{2+}$and (b) the two $(d_{xz},d_{yz})^3(d_{xy},a_{2u})^3a_{1u}^2$ configurations of $[Fe(P)(ImH)_2]^{2+}$: **E** (left) and **F** (right).

TABLE 1: Correlation between the Standard D_{4h} Irreducible Representations and the Irreducible Representations of Lower Order Point Groups of Nonplanar Porphyrins

	point group			
	D_{4h}	D_{2d}		C_{4v}
orbital	planar	ruffled	saddled	domed
metal d orbitals				
xy	b_{2g}	b_2	b_1	b_2
xz/yz	e_g	e	e	e
z^2	a_{1g}	a_1	a_1	a_1
x^2-y^2	b_{1g}	b_1	b_2	b_1
porphyrin HOMOs				
a_{1u}	a_{1u}	b_1	b_1	a_2
a_{2u}	a_{2u}	b_2	b_2	a_1

meshes to allow for a correct description of nonplanar porphyrin distortions. Additional details of the individual calculations, such as the electronic configurations studied, are indicated in the discussion below.

Before the results are presented, it may useful to remind the reader of the symmetry properties of the relevant molecular orbitals of the molecules studied. For a planar D_{4h} metalloporphyrin, the metal d orbitals are all orthogonal to the porphyrin a_{1u} and a_{2u} HOMOs.[44,45] However, for a ruffled D_{2d} metalloporphyrin, the t_{2g}-type metal d_{xy} orbital and porphyrin a_{2u} HOMO both transform as b_2 and indeed overlap in a remarkable manner (discussed previously as well as below).[34−38] As summarized in Table 1, other metal(d)−porphyrin(π) orbital interactions become symmetry-allowed for other kinds of distortion of the metalloporphyrin ring system such as doming and saddling. The t_{2g}-type metal d_{xz} and d_{yz} orbitals form an e pair under D_{2d} symmetry, whereas the porphyrin a_{1u} HOMO transforms as b_1. In the discussion below, we therefore specify the electronic configuration of a particular D_{2d} ruffled six-coordinate low-spin iron porphyrin derivative as follows:

$$(d_{xz},d_{yz})^p(d_{xy},a_{2u})^q a_{1u}{}^r \text{ or } e^p b_2{}^q b_1{}^r$$

where p ($p = 1-4$) is the total number of electrons in d_{xz} and d_{yz} orbitals, q ($q = 1-4$) the total number of electrons in metal d_{xy} orbital and the porphyrin a_{2u} HOMO, and r ($r = 1-2$) the number of electrons in the porphyrin a_{1u} HOMO; the axial ligands define the z direction.

Recapitulation of Earlier Results

To put our new results on $[Fe(P)(Py)_2]^{2+}$ and $[Fe(P)(ImH)_2]^{2+}$ in perspective, we have reinvestigated two molecules we studied previously,[38] namely, $[Fe(P)(Py)_2]^+$ (D_{2d}, $S = {}^1/_2$) and $[Fe(P)(4\text{-CN-Py})_2]^+$ (D_{2d}, $S = {}^1/_2$, 4-CN-Py = 4-cyanopyridine). Two different d-orbital occupancies were examined for each molecule, $(d_{xz},d_{yz})^3(d_{xy},a_{2u})^4a_{1u}^2$ or $e^3b_2{}^4b_1{}^2$ and $(d_{xz},d_{yz})^4(d_{xy},a_{2u})^3a_{1u}^2$ or $e^4b_2{}^3b_1{}^2$, where we have followed the notation described above. Spectroscopic studies indicate that although $[Fe(TPP)(Py)_2]^+$ exhibits the common $(d_{xz},d_{yz})^3(d_{xy},a_{2u})^4a_{1u}^2$ electronic configuration, $[Fe(TPP)(4\text{-CN-Py})_2]^+$ exhibits an unusual $(d_{xz},d_{yz})^4(d_{xy},a_{2u})^3a_{1u}^2$ configuration.[34−37] Our DFT calculations predict almost identical energies for both electronic configurations of $[Fe(P)(Py)_2]^+$ and favor the $(d_{xz},d_{yz})^4(d_{xy},a_{2u})^3a_{1u}^2$ configuration over the $(d_{xz},d_{yz})^3(d_{xy},a_{2u})^4a_{1u}^2$ configuration by ~1.1 kcal/mol for $[Fe(P)(4\text{-CN-Py})_2]^+$. The calculations also predict significant electronic spin populations at the *meso* positions for the $(d_{xz},d_{yz})^4(d_{xy},a_{2u})^3a_{1u}^2$ configurations, resulting from a metal(d_{xy})−porphyrin(a_{2u}) orbital overlap that becomes symmetry-allowed for a ruffled porphyrin. This orbital interaction also leads to a significantly more ruffled geometry for the $(d_{xz},d_{yz})^4(d_{xy},a_{2u})^3a_{1u}^2$ configuration of these two complexes than for the $(d_{xz},d_{yz})^3(d_{xy},a_{2u})^4a_{1u}^2$ configuration. Thus, the *meso* carbons of the $(d_{xz},d_{yz})^4(d_{xy},a_{2u})^3a_{1u}^2$ configuration of $[Fe(P)(Py)_2]^+$ and $[Fe(P)(4\text{-CN-Py})_2]^+$ are both displaced by 0.506 Å relative to the mean porphyrin plane, which may be compared with displacements of 0.262 and 0.244 Å for the $(d_{xz},d_{yz})^3(d_{xy},a_{2u})^4a_{1u}^2$ configuration of the two complexes, respectively. As discussed previously,[38] these results are in good qualitative agreement with the experimental scenario. Tables 2 and 3 present selected optimized geometry parameters and spin populations, respectively, for these complexes. Figure 1 presents the numbering of the different atoms in the complexes studied.

Results and Discussion

Spin-unrestricted DFT calculation were carried out on a number of different plausible electronic configurations of $[Fe(P)(Py)_2]^{2+}$ consistent with an $S = 1$ state, that is, with two more α electrons than β electrons. Two electronic configurations appear to compete as the ground state of the molecule, exhibiting nearly identical energies, namely, a $(d_{xz},d_{yz})^2(d_{xy},a_{2u})^4a_{1u}^2$ or $e^2b_2{}^4b_1{}^2$ configuration (hereafter called configuration **A**) and a $(d_{xz},d_{yz})^3(d_{xy},a_{2u})^3a_{1u}^2$ or $e^3b_2{}^3b_1{}^2$ configuration (hereafter called **B**). Both **A** and **B** may be formally regarded as iron(IV)-like d^4 metal complexes, having $d_{xy}{}^2d_{xz}{}^1d_{yz}{}^1$ and $d_{xy}{}^1d_{xz}{}^2d_{yz}{}^1$ d electron occupancies, respectively. Two additional low-spin Fe(III) porphyrin radical configurations were examined, which may be described as $(d_{xz},d_{yz})^3(d_{xy},a_{2u})^4a_{1u}^1$ or $e^3b_2{}^4b_1{}^1$ (hereafter called **C**) and $(d_{xz},d_{yz})^4(d_{xy},a_{2u})^3a_{1u}^1$ or $e^4b_2{}^3b_1{}^1$ (hereafter called **D**), but these were about 0.3 and 0.35 eV higher, respectively, than either **A** or **B**. Spin-unrestricted calculations on the two C_2 conformations of $[Fe(P)(ImH)_2]^{2+}$ −say **E** and **F**− with unspecified electronic occupations, other than the specification of an excess of two α electrons over β electrons, resulted in a $(d_{xz},d_{yz})^3(d_{xy},a_{2u})^3a_{1u}^2$ configuration, resembling configuration **B** of $[Fe(P)(Py)_2]^{2+}$, in each case. The two conformations exhibited nearly identical energies.

TABLE 2: Selected Optimized Geometry Parameters of the Molecules Studied (See Figure 1 for the Numbering of the Atoms)

complex	configuration	Fe−N_{por} (Å)	Fe−N_{axial} (Å)	z_α (Å)	z_β (Å)	z_{meso} (Å)	ruffling torsion angle (deg)
$[Fe^{IV}(P)(ImH)_2]^{2+}$	**E**	$N_{3,4}$: 1.974 $N_{1,2}$: 2.014	2.010				2.5−3
	F	N_4: 1.966 N_1: 1.982 N_3: 1.982 N_2: 2.034	1.994				10.0−12.6
$[Fe^{IV}(P)(Py)_2]^{2+}$	**A**	1.970	2.053	0.213	0.147	0.365	22.15
	B	1.962	2.038	0.319	0.217	0.530	33.66
	C	1.976	2.044	0.208	0.143	0.363	21.83
	D	1.960	2.038	0.326	0.220	0.552	34.46
$[Fe^{III}(P)(Py)_2]^{+}$	$(d_{xz},d_{yz})^3(d_{xy})^2$	1.991	2.031	0.154	0.105	0.262	16.06
	$(d_{xz},d_{yz})^4(d_{xy})^1$	1.973	2.021	0.306	0.205	0.506	32.26
$[Fe^{III}(P)(4\text{-}CN\text{-}Py)_2]^{+}$	$(d_{xz},d_{yz})^3(d_{xy})^2$	1.992	2.027	0.142	0.096	0.242	14.81
	$(d_{xz},d_{yz})^4(d_{xy})^1$	1.974	2.011	0.306	0.205	0.506	32.24

As may be seen from Table 3, electronic configuration **C** of $[Fe(P)(Py)_2]^{2+}$ exhibits a spin density profile characteristic of a porphyrin A_{1u}-type radical, with a full electron spin distributed over the porphyrin ring. In sharp contrast, configurations **A**, **B**, **E**, and **F** exhibit metal spin populations considerably greater than 1.0 and porphyrin spin populations considerably less than 1.0. Indeed, as alluded to above, these electronic configurations may be formally regarded as d^4 and have significant to substantial Fe(IV) character. Configuration **A** has ∼80% of the overall molecular unpaired spin localized on the metal and therefore may be said to exhibit "substantial" Fe(IV) character; configurations **B**, **E**, and **F** have ∼60% of the overall molecular unpaired spin located on the Fe and therefore may be regarded as having "significant" Fe(IV) character. This electronic-structural description also provides a natural explanation for an S = 1 ground state with an apparently "strong metal−porphyrin ferromagnetic coupling". Had the magnetic orbitals been, say, a d_{yz} orbital on the Fe and an a_{1u} orbital on the porphyrin, as in the case of configuration **C**, the metal−ligand spin coupling might have been expected to be weak, because the metal d_{yz} orbital is orthogonal by symmetry to the porphyrin a_{1u} HOMO.

Figure 2a depicts one of the two degenerate α-spin e HOMOs of configuration **A** of $[Fe(P)(Py)_2]^{2+}$. Figure 2b depicts the α-spin b_2 HOMO of configuration **B**. Parts a and b of Figure 2 denote rather different types of metal−porphyrin orbital interactions. Thus, Figure 2a depicts a relatively ordinary metal(d_π)−porphyrin(p_π) orbital overlap, whereby some 20% of the unpaired spin of the Fe(IV) center is delocalized to the porphyrin. Figure 2b depicts a *ruffling-induced* metal(d_{xy})−porphyrin(a_{2u}) overlap,[38] which is symmetry-forbidden in a planar porphyrin. As mentioned above, we encountered this orbital interaction in our calculations on the $(d_{xz},d_{yz})^4(d_{xy})^1$ or $e^4b_2^1$ configurations of the Fe(III) complexes $[Fe(P)(Py)_2]^+$ and $[Fe(P)(4\text{-}CN\text{-}Py)_2]^+$. This orbital interaction is favored by—or leads to—enhanced ruffling, and configuration **B** of $[Fe(P)(Py)_2]^{2+}$ is indeed substantially more ruffled than configuration **A**, the displacements of the *meso* carbons being 0.365 and 0.530 Å for **A** and **B**, respectively.

Interestingly, although **E** and **F** feature relatively planar porphyrin rings for which the a_{1u} and a_{2u} HOMOs are expected to be orthogonal to the Fe d_π orbitals, an examination of the frontier MOs reveals extensive metal(d_π)−porphyrin(π) orbital overlap. It appears that for these C_2 complexes, even the small deviations from octahedral local symmetry at the metal center suffice to promote extensive metal(d_π)−porphyrin(π) orbital overlap.

A comment may be in order with regard to the reliability of the results reported here. The PW91 functional has been extensively tested on transition metal porphyrins, particularly high-valent metalloporphyrins.[4] However, certain cases have been documented where hybrid functionals such as B3LYP perform somewhat better.[46,47] In other cases involving transition metals, however, the B3LYP functional has been documented to perform poorly.[5] On balance, we believe that the results and conclusions of this paper are indeed sound. We refer the interested reader to our recent calibrations of DFT calculations on prototype transition metal complexes against CASPT2 and CCSD(T) results for an extended discussion of this question.[5]

Finally, efforts are also underway in our laboratory to computationally model the strong $[Fe(porphyrinato)(2\text{-}MeIm)_2]^{2+}$ derivatives studied recently by Nakamura and co-workers.[41,42]

Conclusion

DFT calculations suggest two alternative electronic configurations—a $(d_{xz},d_{yz})^2(d_{xy},a_{2u})^4a_{1u}^2$ or $e^2b_2^4b_1^2$ configuration and a $(d_{xz},d_{yz})^3(d_{xy},a_{2u})^3a_{1u}^2$ or $e^3b_2^3b_1^2$ configuration—as plausible candidates for the ground states of $[Fe(P)(Py)_2]^{2+}$ and $[Fe(P)(ImH)_2]^{2+}$ and, by extension, also for $[Fe(TPP)(1\text{-}MeIm)_2]^{2+}$. On the basis of the calculated energetics, we are unable to say which of these two configurations corresponds to the actual ground state of $[Fe(TPP)(1\text{-}MeIm)_2]^{2+}$. However, these two configurations are predicted to exhibit very different spin density profiles as well as different degrees of macrocycle ruffling; spectroscopic and structural studies are therefore expected to readily distinguish between the two configurations. Both configurations may be formally regarded as d^4 and are low-spin Fe(IV)-like, which provides a natural explanation for the experimentalists' unusual characterization of the S = 1 complex $[Fe(TPP)(1\text{-}MeIm)_2]^{2+}$ as a low-spin Fe(III) porphyrin π-cation radical with strong metal−porphyrin ferromagnetic coupling.

Might these results be biologically relevant, specifically to the question of metal−porphyrin ferromagnetic coupling in peroxidase compound I intermediates? Such a connection may well exist, although it is by no means established. Thus, Deeth[7] as well as we[10] have discussed the possibility that porphyrin radical in horseradish peroxidase compound I may be partially delocalized to the axial histidine ligand of the iron center and this may be a factor that strengthens ferromagnetic coupling in this intermediate. However, the case of chloroperoxidase compound I[13] may serve as an apparent counterexample. Here, the radical appears to be delocalized on the porphyrin and axial

TABLE 3: Gross Atomic Spin Populations and Mulliken Atomic Charges (in Parentheses) of the Molecules Studied (See Figure 1 for the Numbering of the Atoms)

	$[Fe^{V}(P)(ImH)_2]^{2+}$		$[Fe^{V}(P)(Py)_2]^{2+}$				$[Fe^{III}(P)(Py)_2]^{+}$		$[Fe^{III}(P)(4\text{-CN-Py})_2]^{+}$	
atom	**E**	**F**	**A**	**B**	**C**	**D**	$(d_{xz},d_{yz})^3(d_{xy})^2$	$(d_{xz},d_{yz})^4(d_{xy})^1$	$(d_{xz},d_{yz})^3(d_{xy})^2$	$(d_{xz},d_{yz})^4(d_{xy})^1$
Fe	1.326 (0.786)	1.299 (0.819)	1.531 (0.851)	1.196 (0.866)	0.959 (0.825)	0.875 (0.867)	0.953 (0.806)	0.872 (0.850)	0.928 (0.806)	0.823 (0.852)
N_{por}	N_1: −0.002 (−0.431)	N_1: 0.067 (−0.432)	0.036 (−0.457)	0.084 (−0.442)	−0.043 (−0.446)	−0.015 (−0.447)	−0.005 (−0.450)	0.024 (−0.450)	−0.002 (−0.455)	0.030 (−0.453)
	N_3: 0.112 (−0.442)	N_3: 0.067 (−0.432)								
	N_2: −0.002 (−0.431)	N_2: −0.027 (−0.414)								
	N_4: 0.112 (−0.442)	N_4: 0.126 (−0.422)								
C_α	$\alpha_{1,4}$: −0.006 (0.251)	$\alpha_{1,6}$: −0.014 (0.256)	0.001 (0.257)	−0.029 (0.251)	0.151 (0.274)	0.137 (0.270)	0.002 (0.251)	−0.014 (0.244)	0.002 (0.247)	−0.015 (0.241)
	$\alpha_{2,3}$: −0.002 (0.263)	$\alpha_{2,5}$: −0.020 (0.256)								
	$\alpha_{5,8}$: −0.032 (−0.246)	$\alpha_{3,4}$: −0.002 (0.262)								
	$\alpha_{6,7}$: −0.017 (0.256)	$\alpha_{7,8}$: −0.030 (0.249)								
C_β	$\beta_{1,4}$: 0.049 (0.205)	$\beta_{1,6}$: 0.040 (0.213)	0.055 (0.223)	0.019 (0.213)	0.036 (0.219)	0.018 (0.214)	0.015 (0.189)	−0.004 (0.183)	0.017 (0.194)	−0.004 (0.187)
	$\beta_{2,3}$: 0.034 (0.207)	$\beta_{2,5}$: 0.040 (0.222)								
	$\beta_{5,8}$: 0.029 (0.215)	$\beta_{3,4}$: 0.034 (0.212)								
	$\beta_{6,7}$: 0.010 (0.207)	$\beta_{7,8}$: 0.002 (0.218)								
C_{meso}	m_1: 0.090 (0.166)	m_1: 0.098 (0.143)	−0.008 (0.140)	0.158 (0.169)	−0.058 (0.136)	−0.000 (0.153)	−0.005 (0.109)	0.058 (0.132)	−0.005 (0.110)	0.068 (0.135)
	m_3: 0.090 (0.166)	m_3: 0.100 (0.140)								
	m_4: 0.090 (0.170)	m_4: 0.098 (0.143)								
	m_2: 0.089 (0.178)	m_2: 0.100 (0.140)								
N_{axial}	−0.014 (−0.333)	−0.014 (−0.326)	−0.037 (−0.348)	−0.018 (−0.357)	−0.022 (−0.355)	−0.015 (−0.350)	−0.022 (−0.347)	−0.014 (−0.343)	−0.022 (−0.344)	−0.012 (−0.344)

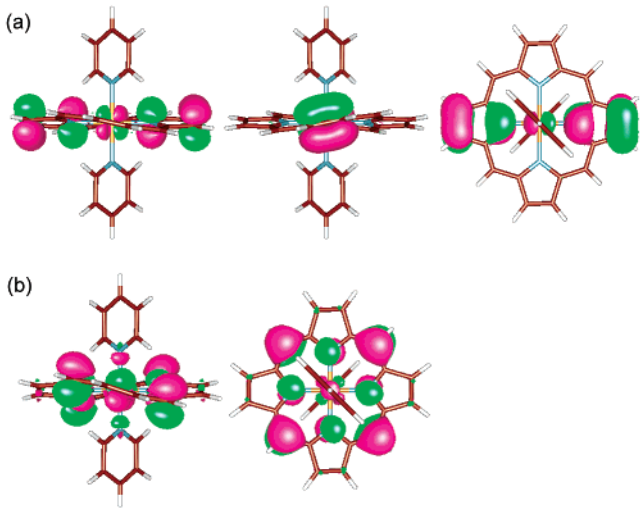

Figure 2. (a) One of the two degenerate α-spin e HOMOs of configuration **A** of $[Fe(P)(Py)_2]^{2+}$. (b) α-Spin b_2 HOMO of configuration **B**: note the ruffling-induced metal(d_{xy})−porphyrin(a_{2u}) orbital interaction.

cysteinate ligands, but this results in an antiferromagnetic coupling with the ferryl unit, resulting in a unique overall $S = {}^1/_2$ state.

Acknowledgment. This work was supported by the Research Council of Norway and the National Research Fund of the Republic of South Africa.

Supporting Information Available: Optimized Cartesian coordinates. This material is available free of charge via the Internet at http://pubs.acs.org.

References and Notes

(1) For a review on high-valent heme intermediates, see, e.g.: Terner, J.; Gold, A.; Weiss, R.; Mandon, D.; Trautwein, A. X. *J. Porphyrin Phthalocyanines* **2001**, *5*, 357−364.

(2) For a review on high-valent nonheme diamond-core intermediates, see: Que, L.; Tolman, W. B. *Angew. Chem., Int. Ed.* **2002**, *41*, 1114−1137.

(3) For a review on the applications of DFT to metalloenzymes, see: Siegbahn, P. E. M.; Blomberg, M. R. A. *Chem. Rev.* **2000**, *100*, 421−437.

(4) For a review on DFT calculations on high-valent metalloporphyrins and related complexes, see: Ghosh, A.; Steene, E. *J. Biol. Inorg. Chem.* **2001**, *6*, 739−752.

(5) For a review on the limitations of DFT vis-à-vis transition metal calculations, see: Ghosh, A.; Taylor, P. R. *Curr. Opin. Chem. Biol*. **2003**, *7*, 113−124. For another relevant study, see: Ghosh, A.; Persson, B. J.; Taylor, P. R. *J. Biol. Inorg. Chem.* **2003**, *8*, 507−511.

(6) Vangberg, T.; Lie, R.; Ghosh, A. *J. Am. Chem. Soc*. **2002**, *124*, 8122−8130.

(7) Ghosh, A.; Almlöf, J.; Que, L., Jr. *J. Phys. Chem*. **1994**, *98*, 5576−5579.

(8) Kuramochi, H.; Noodleman, L.; Case, D. A. *J. Am. Chem. Soc*. **1997**, *119*, 11442−11451.

(9) Deeth, R. J. *J. Am. Chem. Soc*. **1999**, *121*, 6074−6075.

(10) Vangberg, T.; Ghosh, A. *J. Am. Chem. Soc.* **1999**, *121*, 12154−12160.

(11) Harris, D. L. *Curr. Opin. Chem. Biol*. **2001**, *5*, 724−735.

(12) Green, M. T. *J. Am. Chem. Soc*. **1998**, *120*, 10772−10773.

(13) Green, M. T. *J. Am. Chem. Soc*. **1999**, *121*, 7939−7940.

(14) Green, M. T. *J. Am. Chem. Soc*. **2001**, *123*, 9218−9219.

(15) Ghosh, A.; Steene, E. *J. Inorg. Biochem*. **2002**, *91*, 423−436.

(16) Ghosh, A.; Gonzalez, E.; Vangberg, T.; Taylor, *J. Porphyrin Phthalocyanines* **2001**, *5*, 345−356.

(17) Dey, A.; Ghosh, A. *J. Am. Chem. Soc*. **2002**, *124*, 3206−3207.

(18) Ghosh, A.; Gonzalez, E. *Israel J. Chem.* **2000**, *40*, 1−8.

(19) Steene, E.; Wondimagegn, T.; Ghosh, A. *J. Phys. Chem. B* **2001**, *105*, 11406−11413.

(20) Tangen, E.; Ghosh, A. *J. Am. Chem. Soc*. **2002**, *124*, 8117−8121.

(21) Zakharieva, O.; Schünemann, V.; Gerdan, M.; Licoccia, S.; Cai, S.; Walker, F. A.; Trautwein, A. X. *J. Am. Chem. Soc.* **2002**, *124*, 6636−6648.

(22) Ghosh, A.; Wondimagegn, T.; Gonzalez, E.; Halvorsen, I. *J. Inorg. Biochem.* **2000**, *78*, 79−82.

(23) Wondimagegn, T.; Ghosh, A. *J. Am. Chem. Soc.* **2001**, *123*, 1543−1544.

(24) Ghosh, A.; Wondimagegn, T.; Parusel, A. B. J. *J. Am. Chem. Soc.* **2000**, *122*, 5100−5104.

(25) Goff, H. M.; Phillippi, M. *J. Am. Chem. Soc.* **1983**, *105*, 7567−7571.

(26) Mathews, F. S.; Czerwinsky, E. W.; Argos, P. In *The Porphyrins*; Dolphin, D., Ed.; Academic Press: New York, 1979; Vol. VII, p 108.

(27) Pierrot, M.; Haser, R.; Frey, M.; Payan, F.; Astier, J. P. *J. Biol. Chem.* **1982**, *257*, 14341.

(28) Higuchi, Y.; Kusunoki, M.; Matsuura, Y.; Yasuoka, N.; Kakudo, M. *J. Mol. Biol.* **1984**, *172*, 109.

(29) Widger, W. R.; Cramer, W. A.; Herrmann, R. G.; Trebst, A. *Proc. Natl. Acad. Sci. U.S.A.* **1984**, *81*, 674.

(30) Badcock, G. T.; Widger, W. R.; Cramer, W. A.; Oertling, W. A.; Metz, J. *Biochemistry* **1985**, *24*, 3638.

(31) Chiu, J. T.; Loewen, P. C.; Switala, J.; Gennis, R. B.; Timkovich, R. J. *J. Am. Chem. Soc.* **1989**, *111*, 7046.

(32) Lorence, R. M.; Gennis, R. B. *J. Biol. Chem.* **1989**, *264*, 7135.

(33) Chang, C. K.; Wu, W. *J. Biol. Chem.* **1986**, *261*, 8593.

(34) Safo, M. K.; Walker, F. A.; Raitsimring, A. M.; Walters, W. P.; Dolata, D. P.; Debrunner, P. G.; Scheidt, W. R. *J. Am. Chem. Soc.* **1994**, *116*, 7760−7770.

(35) Walker, F. A.; Nasri, H.; Turowska-Tyrk, I.; Mohanrao, K.; Watson, C. T.; Shokhirev, N. V.; Debrunner, P. G.; Scheidt, W. R. *J. Am. Chem. Soc.* **1996**, *118*, 12109−12118.

(36) Geze, C.; Legrand, N.; Bondon, A.; Simonneaux, G. *Inorg. Chim. Acta* **1992**, *195*, 73−76.

(37) Guillemot, M.; Simonneaux, G. *J. Chem. Soc., Chem. Commun.* **1995**, 2093−2094.

(38) Ghosh, A.; Gonzalez, E.; Vangberg, T. *J. Phys. Chem. B* **1999**, *103*, 1363−1367.

(39) Johansson, M. P.; Sundholm, D.; Gerfen, G.; Wikström, M. *J. Am. Chem. Soc.* **2002**, *124*, 11771−11780.

(40) Gans, P.; Buisson, G.; Duée, E.; Marchon, J. C.; Erler, B. S.; Scholz, W. F.; Reed, C. A. *J. Am. Chem. Soc.* **1986**, *108*, 1223−1234.

(41) Ikeue, T.; Ohgo, Y.; Nakamura, M. *Chem. Commun.* **2003**, 200−221.

(42) Nakamura, M.; Kawasaki, Y. *Chem. Lett.* **1996**, 805−806.

(43) The ADF program was obtained from Scientific Computing and Modelling NV, Department of Theoretical Chemistry, Vrije Universiteit, 1081 HV Amsterdam, The Netherlands.

(44) Gouterman, M. In *The Porphyrins*; Dolphin, D., Ed.; Academic: New York, 1978; Vol. III, Part A, Physical Chemistry, pp 1−165.

(45) Ghosh, A. *Acc. Chem. Res.* **1998**, *31*, 189−198.

(46) Loew, G. H.; Harris, D. L. *Chem. Rev.* **2000**, *100*, 407−420.

(47) Salomon, O.; Reiher, M.; Hess, B. A. *J. Chem. Phys.* **2002**, *117*, 4729−4737.